Available online at www.sciencedirect.com
ScienceDirect
Journal of the European Ceramic Society 28 (2008) 69–76
www.elsevier.com/locate/jeurceramsoc

Microstructure and property evaluation of barium aluminosilicate glass–ceramic sealant for anode-supported solid oxide fuel cell

Saswati Ghosh, P. Kundu, A. Das Sharma, R.N. Basu *, H.S. Maiti

Fuel Cell and Battery Section, Central Glass & Ceramic Research Institute, Kolkata 700032, India

Received 8 March 2007; received in revised form 18 May 2007; accepted 24 May 2007
Available online 13 August 2007

Abstract

Several glass compositions based on the barium aluminosilicate system have been investigated for their application as sealant for solid oxide fuel cell (SOFC). The developed glasses were characterized through measurement of different properties, viz. coefficient of thermal expansion (CTE), glass transition temperature (T_g), dilatometric softening temperature (T_d), crystallization behavior during prolonged heat-treatment, electrical resistivity measurement, microstructural studies, etc. In addition, bonding behavior between zirconia electrolyte and metallic interconnect in sandwiched condition has also been investigated to find out their suitability as sealant for SOFC. Microstructural investigation revealed a well-adhered bonding between the electrolyte and the metallic interconnect. The optimized glass composition also showed a high resistivity ($\sim 10^5\ \Omega$ cm) at the SOFC operation temperature ($\sim$800 °C).

Keywords: Solid oxide fuel cell; Glass–ceramics; Electron microscopy; Thermal expansion

1. Introduction

Solid oxide fuel cells (SOFCs) provide advantages of high energy conversion efficiency, such as heat utilization and ability to use a variety of fuels, due to their high operating temperature in the range between 800 and 1000 °C.[1–3] An SOFC consists of three essential components: a porous cathode, a dense electrolyte and a porous anode. The most commonly used materials are lanthanum strontium manganite as cathode, yttria stabilized zirconia (YSZ) as the electrolyte and Ni–YSZ cermet as anode.[4,5] For practical applications, however, several such cells are generally stacked together to achieve a higher power output. Two basic designs are available for the SOFC stack: tubular and planar. Among these two designs, the state-of-the-art anode-supported planar design[6,7] has been adopted by most of the leading SOFC developers that can be operated at an intermediate temperature range between 700 and 800 °C (IT-SOFC), so that ceramic interconnects can be replaced by metallic interconnects.[4,5] However, for a planar SOFC stack, gas-tight seals must be applied along the edges of each cell and between the cell stack and gas manifolds in order to avoid intermixing of fuel gas (on anode side) and air (on cathode side). Thus the development of such gas-tight and durable sealant is one of the major technological challenges for the planar SOFC stack developers. Generally, the sealants for SOFC must meet the following requirements: (a) matching coefficient of thermal expansion (CTE) with other SOFC components; (b) high electrical resistivity to avoid short circuiting between different layers of the stack; (c) good thermo-chemical compatibility with relevant SOFC components (i.e., no harmful reaction with joining components); (d) high chemical stability and low vapor pressure in both reducing and oxidizing atmospheres; (e) must be non-spreading to the adjoining fuel cell components at the operating temperature (f) should have deformability but must be able to withstand a slight overpressure; (g) should be able to survive even thousands of thermal cycles during operation at elevated temperature.[4,5,8–11]

In general, glass or glass–ceramic sealants can, in principle, meet almost all the above-mentioned requirements. One of the major advantages of these variety of sealants is that the chemical compositions of the glass can be tailored so as to control some important physical properties such as matching CTE, appro-

* Corresponding author. Tel.: +91 33 24733469; fax: +91 33 24730957.
E-mail address: rnbasu@cgcri.res.in (R.N. Basu).

0955-2219/$ – see front matter © 2007 Elsevier Ltd. All rights reserved.
doi:10.1016/j.jeurceramsoc.2007.05.008

priate viscosity, etc. Till date, many studies have been carried out over the application of glasses or glass–ceramics as suitable sealants for high temperature electrochemical devices e.g., SOFCs.[8–26] All three of the primary glass forming oxides viz., B_2O_3, P_2O_5 and SiO_2 have been investigated individually along with other constituents as potential SOFC seals. However, best results have been reported only for compositions based on silica. While the alkali silicate glasses tend to be very reactive towards other SOFC components[8], alkaline earth aluminosilicate glasses have yielded promising results.[16–26] But in most of the earlier reports[16–21], major emphasis was given to characterize the developed glass compositions through various characterization techniques such as DTA, CTE measurements, XRD, etc. Moreover, in all these cases, the joining of the developed glass seals was studied only with zirconia electrolyte having sealing temperatures varied within 900–1000 °C, which is much above the operating temperature of the state-of-the art anode-supported SOFC (700–800 °C), where special steel such as ferritic steel is used as interconnect.[18,22] There are some report[23–26] on the development of $BaO–CaO–Al_2O_3–SiO_2$ (BCAS) based glass systems, which have a relatively high CTE quite close to that of commercial metallic interconnect (Crofer22APU) having CTE $\sim 12.1 \times 10^{-6}$/K.[24,26] In all these works, the chemical interaction of the glass with the alloy was studied and so far as the sealing behavior of the glass is concerned, only the metal–metal sealing was investigated. Recently we have reported application of a compositionally graded glass in the BCAS system which was found to be effective for joining dissimilar materials viz., metal and ceramic.[27] However, to the best of the authors' knowledge, no study has been made till date to develop a suitable glass based seal of single composition, which can simultaneously join YSZ electrolyte on one side, and Crofer22APU on the other, which, in turn, is necessary for development of anode-supported working stack.

The present study dealt with the development of suitable glass–ceramic sealants based on $BaO–Al_2O_3–SiO_2$ (BAS) system for joining dissimilar materials such as Crofer22APU and YSZ, at relatively lower sealing temperature (~850 °C), especially suitable for anode-supported planar SOFCs operating between 750 and 800 °C. To estimate the applicability of these glasses as sealants, their thermal properties, crystallization behavior, microstructure upon different heat-treatment schedule and the overall bonding characteristics of the glass sandwiched between ceramic (YSZ) electrolyte and metallic (Crofer22APU) interconnect were investigated. Finally, within the composition ranges studied during the present investigation, an optimum composition has been selected that could act as a useful sealing material for SOFC.

2. Experimental

Chemical compositions of the glasses studied during the present work are given in Table 1. To prepare a suitable glass sealing composition, B_2O_3 and SiO_2 were chosen as glass formers wherein B_2O_3/SiO_2 ratio was kept at around 0.55. Other ingredients such as BaO was added to increase the CTE, La_2O_3 to control the viscosity and Al_2O_3 to prevent rapid crystallization during heat-treatment as well as to control the surface tension of the glass.[28,29]

Table 1
Chemical compositions of the developed glasses

Glass ID	Chemical composition (wt.%)				
	BaO	La_2O_3	Al_2O_3	B_2O_3	SiO_2
G1	46.5	14.0	8.8	12.5	18.2
G2	50.3	10.5	9.6	10.9	18.8
G3	49	14.5	9.1	9.1	18.3

2.1. Glass preparation

The raw materials for preparing the glass batches (Table 1) were made from reagent grade $BaCO_3$ (E-Merck, India), Al_2O_3 (E-Merck, India), $La(NO_3)_3{\cdot}6H_2O$ (Indian Rare Earth Ltd.), H_3BO_3 (E-Merck, India), and SiO_2 (quartz). The thoroughly mixed batches were taken in a Pt–Rh (10%) crucible and melted in an electric furnace, with occasional stirring, at 1400 °C for 2 h. After 2 h, one part of the melts were poured into cast iron mold preheated to about 550 °C and subsequently annealed at around 600 °C for 1 h followed by slow cooling (~1 °C/min) to room temperature. The bulk glasses, thus obtained, were cut into cylindrical shaped specimens (25 mm length and 6 mm diameter) for CTE measurements. The remaining parts of the melts were used for making frits. For this purpose, the melts were quenched by pouring into ice-cooled water, rinsed with acetone and then dried at 80 °C for 24 h. The glass frits were wet milled in acetone in an agate mortar, dried and then sieved through stainless steel mesh to collect powders of size less than 20 μm for subsequent thick film paste preparation.

2.2. Glass and glass–ceramics characterization

The thermal properties of the glass powders, such as glass transition temperature (T_g) and crystallization temperature (T_c) were determined in air using a differential thermal analyzer (DTA) (Shimadzu DTA 40, Japan). The CTEs along with dilatometric softening temperature (T_d) and T_g of the annealed cylindrical glass samples were determined from dilatometric measurements using a dilatometer (Netzsch DIL 402C, Germany). The as-prepared glass powders and the heat-treated powders (fused at 850 °C and subsequently heat-treated at 800 °C for 3, 10, 50 and 100 h) were tested using a X-ray diffractometer (Phillips PW 1710, Holland) with Cu Kα radiation to confirm the amorphous nature (in the as-prepared glass) and to identify the crystalline phases (in the heat-treated glass). In order to show the changes in CTE values of the glass–ceramics during long-term operation, dilatometric measurements were also performed on the rectangular (25 mm × 10 mm × 4 mm) glass samples heat-treated at 800 °C for 10, 50 and 100 h. An Impedance Analyzer (Solartron SI 1260, UK) was used to measure the electrical resistivities of sintered glass–ceramic pellets within the 600 and 800 °C between the frequency ranges of 0.1 Hz to 1 MHz.

2.3. Joining of YSZ electrolyte and Crofer22APU using the glass paste

For application of the glass in the form of thick film, the powder was blended with a suitable organic vehicle to form a viscous paste. The paste was then screen printed on the flat surface of steel plate, Crofer22APU (1 cm × 1 cm × 1 mm), as well as on anode-supported YSZ electrolyte using a semi automatic screen-printing machine (Ming Tai Company 450B, Taiwan). Prior to application of the glass paste, the substrates were thoroughly cleaned in acetone using an ultrasonic bath for 10 min followed by over drying. The joining of the samples was carried out by placing the YSZ surface of the anode-supported electrolyte on top of the metal with the screen-printed glass sandwiched in between. The whole assembly was then put inside a furnace with the metal sample below. Finally a dead load of about 100 g is placed on top of the ceramic sample. The sample was then heated to 850 °C with a relatively slow heating rate (50 °C/h) and kept at that temperature for 1 h. The furnace temperature was then brought down to the SOFC operation temperature (800 °C), heat-treated at that temperature for various period of time (1–100 h) and finally cooled down to room temperature with a cooling rate of 200 °C/h.

2.4. Microstructural studies of YSZ–glass–Crofer22APU interfaces

In order to evaluate the quality of the glass joints at the two different interfaces (YSZ–glass and glass–Crofer22APU) and to investigate the effect of heat-treatment on the corresponding microstructure, polished cross sections of the specimens were examined using optical microscope (Olympus GX71, Japan) and scanning electron microscope (Leo 430i, UK). Particular emphasis was given to examine the formation of any defects (e.g., morphological changes, etc.), if any at the respective interfaces.

3. Results and discussion

The physical property are almost identical for all the glasses developed within the composition range (Table 1) but on the basis of our preliminary microstructural studies of the joined interfaces (both with the YSZ and Crofer22APU) G1 glass was found to be very promising. Hence, this particular glass composition has been referred extensively in this study.

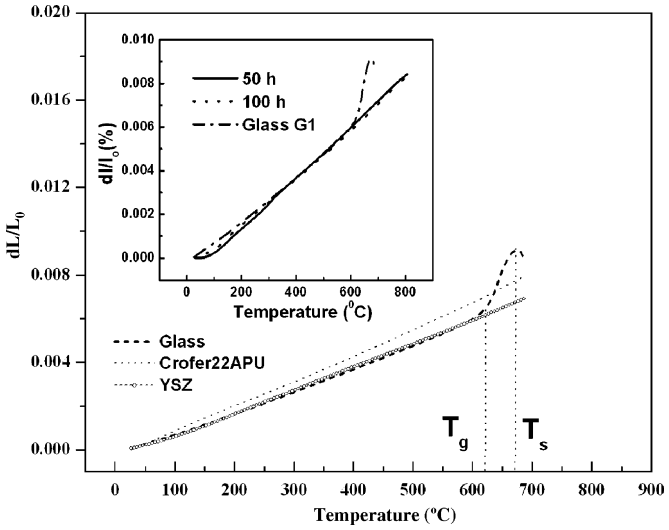

Fig. 1. Comparison of thermal expansion for G1 glass and glass–ceramics (sintered at 800 °C for 50 and 100 h) with YSZ and Crofer22APU (metallic interconnect).

3.1. Physical properties of the developed glasses

All the physical and thermal properties, as obtained from dilatometric study of the developed $BaO–Al_2O_3–SiO_2$ (BAS) glasses, are summarized in Table 2. The T_g values for the developed glasses lie within the temperature range 620–630 °C, which is below the SOFC operating temperature. The CTE values of all these glasses (∼(10.85 to 11.0) × 10^{-6} K^{-1}) from room temperature to T_g and of all these corresponding glass–ceramics from room temperature to 800 °C ((10.5–12.1) × 10^{-6} K^{-1}) are in the same range as that of other cell components, zirconia electrolyte in particular. The results also indicate that T_g, T_d and CTEs are almost independent of the change in BaO content under constant B_2O_3/SiO_2 ratio. Similar behavior was observed by other workers while studying with borosilicate glasses.[8,18] Although the density of all the glasses was almost same (∼4.0 g/cm^3), the G1 glass exhibited the highest CTE value of ∼11.0 × 10^{-6} K^{-1}.

A typical linear expansion curve for the same glass (G1) is shown in Fig. 1 and compared with that of CTE of YSZ and Crofer22APU. The slope of the curve between T_g and T_d shows a dramatic increase in expansion just before the glass structure deforms by viscous flow. When fuel cell stacks are cooled to room temperature, stresses begin to develop as the temperature drops below T_g and with further decrease in temperature, the stress enhances significantly due to the thermal expansion mismatch. Therefore, to minimize the total stress produced, the T_g

Table 2
Physical properties of the developed glasses

Glass ID	T_g (°C)	T_c (°C)	T_d (°C)	Density (g/cm^3)	CTE within RT – T_g (×10^{-6} K^{-1})	CTE within RT – 800 °C (heat-treated at 800 °C for 50 h) (×10^{-6} K^{-1})	CTE within RT – 800 °C (heat-treated at 800 °C for 100 h) (×10^{-6} K^{-1})
G1	625.8	745.7	675.4	4.1	11.0	10.85	10.81
G2	621.6	735.4	669	4.0	10.8	9.514	10.13
G3	630.2	757.7	681	4.1	10.9	11.21	10.90

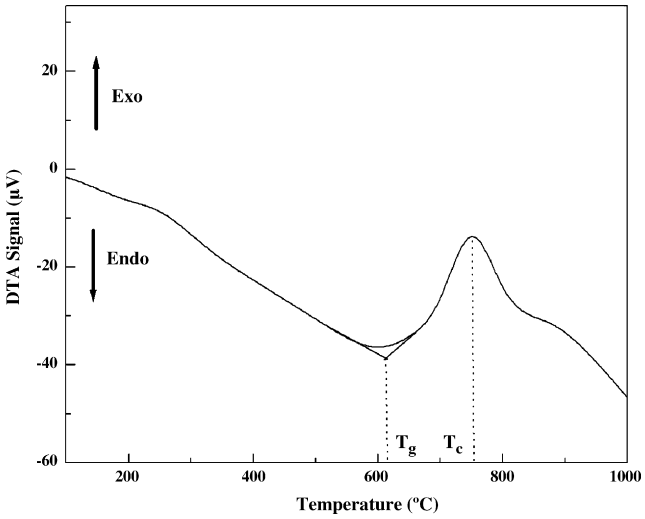

Fig. 2. DTA plot of G1 glass.

at which the viscosity equals to 10^{13} to $10^{13.6}$ dPa s, should be as low as practicable[30] with adequate rigidity at the cell operating temperature of around 800 °C. Fig. 1 also reveals that the difference in CTE between the optimized glass G1 and YSZ electrolyte is small exhibiting a thermal expansion mismatch within 5% below T_g. It should be noted that the difference in CTE between the G1 glass and Crofer22APU is also relatively less and lies below 10% mismatch. The stress arising from the CTE mismatch can be tolerated by the sealant at the cell operating temperature where the stress is being released by viscous flow. The linear thermal expansion behavior of the heat-treated glass–ceramics at 800 °C for 50 and 100 h (shown in the inset of Fig. 1) as compared with the parent glass shows that there is no substantial change in CTE values during prolong crystallization. Hence it can be inferred from this result that though almost complete crystallization occurred during long-term heat-treatment (e.g., 100 h) even then the sealant is compatible with the adjoining cell component like YSZ and Crofer22APU, which ultimately leads to the thermal and thermo-mechanical stability of the sealant during long-term operation.

DTA plot for the same glass composition is shown in Fig. 2. The endothermic peak between the temperature range of 620 and 630 °C is due to glass transition and the broad exothermic peak between 750 and 760 °C is due to crystallization of the glass. No phase transformation occurs at lower temperature. The DTA performed on the other glasses also showed similar type of results and hence is not shown separately.

3.2. Determination of viscosity of G1 glass

The method of calculating viscosity from thermal expansion is quite convenient for the viscosity measurement and has been reported by Wang et al.[31]

From the thermal expansion curve (Fig. 1), the T_d and T_g can be obtained as 948.4 and 898.8 K, respectively. According to the simple liquid theory (Mott and Gurney)[31], there is a relationship between pseudo-critical temperature (T_k) and the absolute melting point (T_m)

$$\frac{T_k}{T_m} = \frac{2}{3} \quad \text{(i)}$$

Beaman[32–34] showed that this rule could be applied on glass–ceramics and there the terms T_k and T_m of Eq. (i) can be replaced with T_g and liquid temperature (T_l), respectively of the glass. Thus Eq. (i) becomes

$$\frac{T_g}{T_l} = \frac{2}{3} \quad \text{(ii)}$$

Hence T_l can be calculated as $T_l = 1348.2$ K. The viscosity values (η) at T_g, T_d and T_l are fixed and independent of materials and are reported[30,31] to be $10^{13.6}$, $10^{11.3}$ and 10^6 dPa s, respectively, at these temperatures. Thus, for the present case according to Vogel–Fulcher–Tamman (VFT) equation.[28,29]

$$\log \eta = A + \frac{B}{T - T_0} \quad \text{(iii)}$$

where A, B and T_0 are all constants.

It is possible to determine all these constants by substituting values for T_g, T_d and T_s in Eq. (iii). Therefore, Eq. (iii) can be modified as

$$\log \eta = 2.96 + \frac{1914.67}{T - 718.89} \quad \text{(iv)}$$

The viscosity–temperature curve of the glass G1 calculated using Eq. (iv) has been shown in Fig. 3. The viscosity value as determined at the sealing temperature (850 °C) is $\sim 10^{7.96}$ dPa s, which is well within the required viscosity value of 10^6 to 10^9 dPa s for sealing applications.[35]

3.3. X-ray diffraction for crystallization study

It is quite evident that, glass–ceramics, which can be prepared by the controlled crystallization of glasses, exhibit superior mechanical properties to glasses and can have various CTE values depending on the type of precipitated crystalline phases

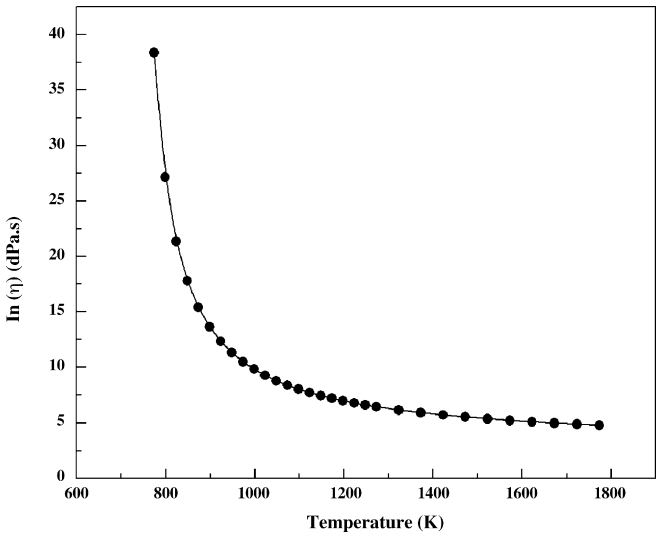

Fig. 3. Temperature dependence of viscosity for G1 glass.

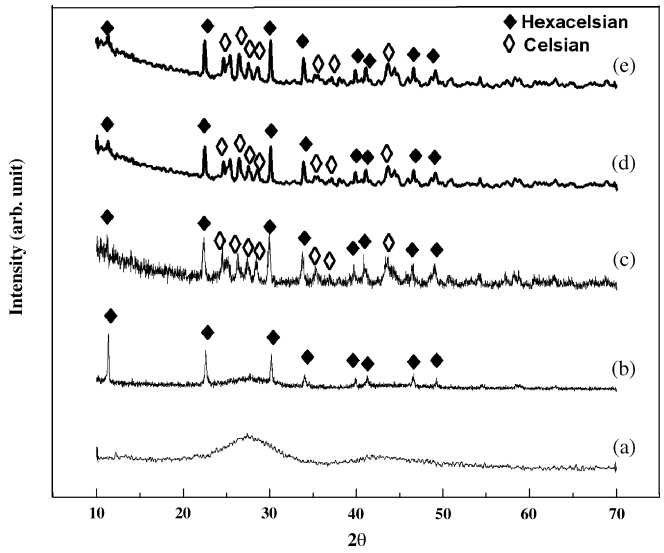

Fig. 4. XRD pattern of the G1 glass heat-treated at 800 °C for different duration of time (a) glass frit without heat-treatment, (b) 3 h, (c) 10 h, (d) 50 h and (e) 100 h.

and their volume fraction in the glass matrix.[18] Glass–ceramics also show higher chemical stability than glasses, especially, under SOFC operating conditions.[36,37] Therefore, the glasses developed in the present investigation were subjected to long-term heat-treatment at 800 °C to study crystallization behavior and any further microstructural changes during prolong thermal operation.

Fig. 4 shows the XRD pattern of the G1 glass, heat-treated at 800 °C for different period of time. The other glasses (Table 1) in this work follow the same trend. The as-prepared glass was found to be X-ray amorphous and they exhibited a broad halo in the XRD pattern (Fig. 4a). As heat-treatment (at 800 °C) goes on, the main crystalline phases precipitated were hexacelsian ($BaAl_2Si_2O_8$), a polymorph of celsian. The high temperature phase, hexacelsian forms metastably after heat-treatment at 800 °C for 3 h (Fig. 4b) and always crystallizes out first in these BAS glasses. When the glasses were heat-treated for longer

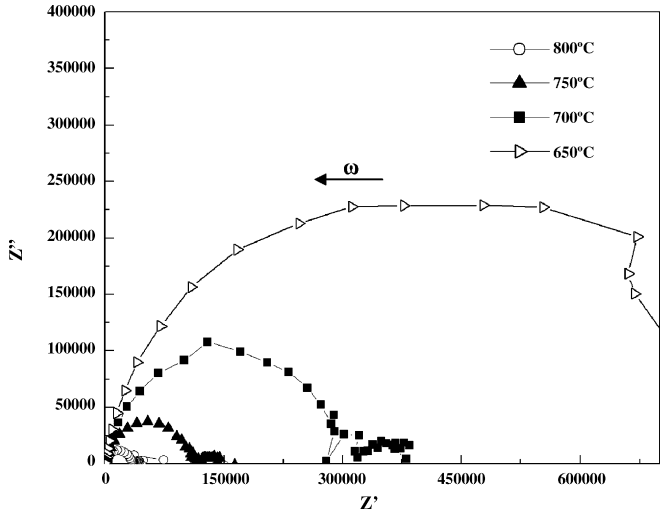

Fig. 5. Complex plane impedance plot of developed glass–ceramic.

Table 3
Variation of electrical resistivity with temperature for G1 glass

Temperature (°C)	Electrical resistivity (Ω cm)
650	1.95×10^7
700	2.88×10^6
750	1.15×10^6
800	3.84×10^5

period of time (10, 50 and 100 h), the hexacelsian phase begins to transform to the monoclinic celsian phase as the latter is thermodynamically stable below ~1590 °C. The formation of celsian phase is, however, undesirable for SOFC sealing application as the same has a very low CTE of $\sim 2.29 \times 10^{-6}\,K^{-1}$ in between 30 and 1000 °C. The hexacelsian phase, on the contrary, has a relatively higher CTE value of $\sim 8 \times 10^{-6}\,K^{-1}$ within 30–1000 °C and is more compatible with the parent glasses compared to celsian in terms of CTE mismatch. Therefore, crystallization of hexacelsian is always desirable in the preparation of glass sealant for SOFCs, whereas, rapid and progressive transformation from hexacelsian to celsian is considered undesirable. Fortunately, the transformation of hexacelsian to celsian is very sluggish. According to Drummond et al.[38] the crystal structure of hexacelsian contains infinite two dimensional hexagonal sheets consisting of two layers of $(Al,Si)O_4$ tetrahedra. Celsian consists of three dimensional feldspar structure in which all four corners of silica tetrahedra are shared forming a three dimensional network. The transformation of hexacelsian to celsian would require the creation of a three dimensional network from a two dimensional structure of hexacelsian as well as rearrangement of the Ba-sites. This would require breaking and forming of Al–O and Si–O bonds. Due to this kinetic barrier, the transformation of hexacelsian to celsian is very slow. The fact that there is practically no change in peak intensity corresponding to the celsian phase in the XRD patterns even much after 50 h of heat-treatment (Fig. 4d and e) also supports the above-mentioned proposition.

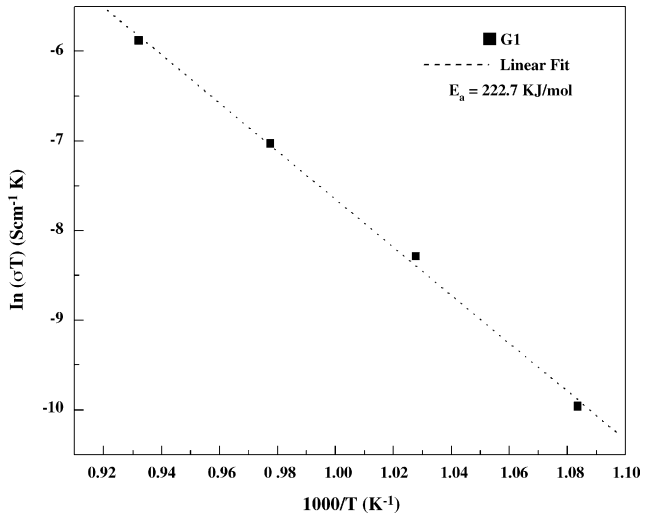

Fig. 6. Variation of electrical conductivity with temperature for developed glass–ceramic.

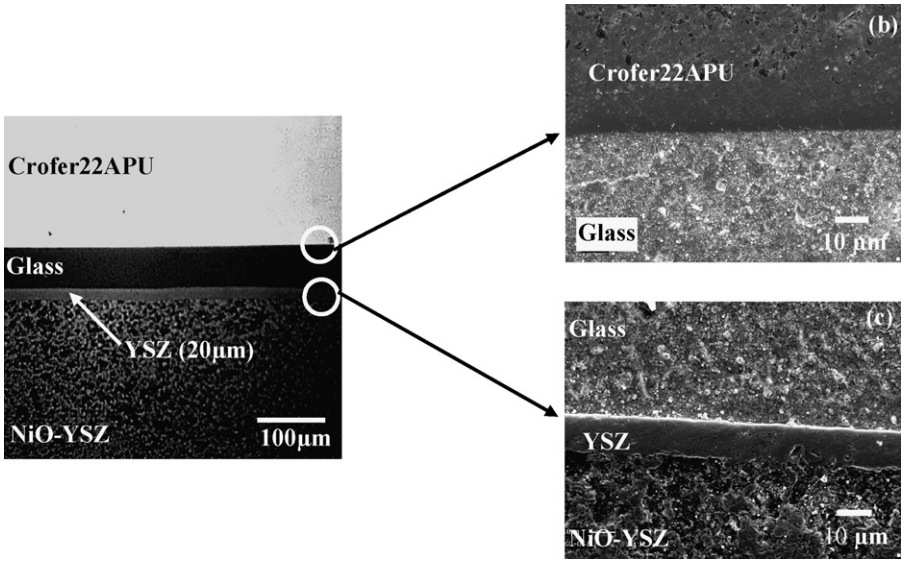

Fig. 7. Sealing of anode-supported cell with Crofer22APU (metallic interconnect) and closure view of (a) metal/glass interface and (b) glass/YSZ interfaces.

3.4. Variation of electrical resistivity with temperature

Fig. 5 represents the complex plane impedance plot of the G1 glass at operating temperatures ranging from 600 to 800 °C and the corresponding resistivity values at different temperatures are given in Table 3. The decrease in resistivity values with increasing temperature could be due to ionic conductivity associated with the migration of Ba^{2+} ions.[39] However, the measured resistivity value at 800 °C ($\sim 10^5\ \Omega$ cm) corresponding to the SOFC operating temperature, is much higher than that reported by others.[4,31]

A linear plot of log(σT) versus 1/T confirms the Arrhenius behavior which is governed by the following well known equation:

$$\sigma = \frac{A}{T} \exp\left(-\frac{E_a}{kT}\right) \quad \text{(v)}$$

where A is a pre-exponential factor, k the Boltzmann constant, T the absolute temperature and E_a is the activation energy for conduction. From the slope of the plot (Fig. 6), the activation energy is calculated to be ~223 kJ/mol that is very close to the reported value of 206 kJ/mol for a barium aluminosilicate (BAS) glass.[39]

3.5. Bonding behavior of G1 glass and effect of heat-treatment on microstructure

As discussed earlier, the CTE value of G1 glass ($\sim 11.0 \times 10^{-6}\ K^{-1}$) is closest to that of the Crofer22APU ($\sim 12.1 \times 10^{-6}\ K^{-1}$) and, at the same time, not far off from the CTE of YSZ electrolyte ($\sim 10.8 \times 10^{-6}\ K^{-1}$). Therefore, it is expected that this glass would result in good adhesion between the glass-electrolyte as well as the glass-interconnect joints. It was indeed found that in the sandwiched sample consisting of YSZ–glass (G1)–Crofer22APU, the G1 glass adhered well both with the metal as well as that of the YSZ under the optimized sealing conditions of the present work. This is evident from the corresponding optical images and the scanning electron microphotographs (SEM) as shown in Fig. 7. A defect free structure, devoid of any major or microcracks at the interfaces, was observed for both the joints (Fig. 7a and b).

The SEM microphotographs of G1 glass heat-treated at 800 °C for different periods of time were shown in Fig. 8. It can be clearly seen that after heat-treatment for 10 h, a large number of crystals grow as spherulites and some of these spherulites grows into a lathlike structure (Fig. 8a). On the other hand, after heat-treatment at the same temperature for a prolonged period of 50 h, the spherulites as well as the lath grow in size and some

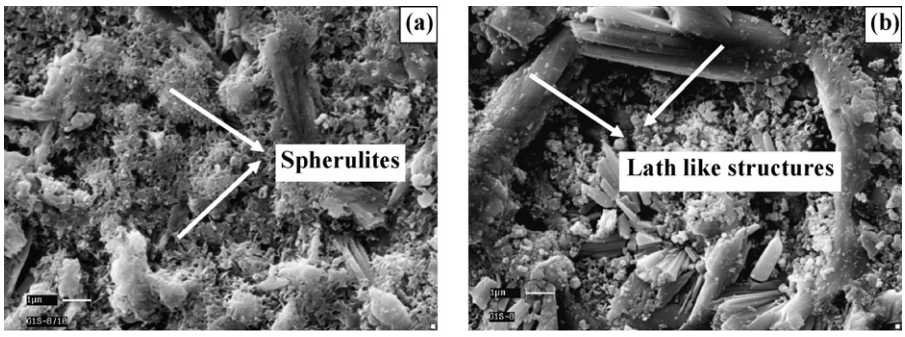

Fig. 8. Microstructure of the developed glass–ceramic specimens heat-treated at 800 °C for (a) 10 h and (b) 50 h.

of the lathlike structure formed in the early stage gets transformed into elongated rod shaped structure (Fig. 8b), indicating enhanced ceramization of the parent glass.

4. Conclusions

Glass–ceramic system of $BaO–Al_2O_3–SiO_2$ (BAS) was evaluated as potential SOFC sealants. The CTEs were found to be well matched with the zirconia electrolyte although there was less than 10% mismatch with the Crofer22APU (interconnect metal), which was within the tolerable limit for application as a sealing material. The heat-treatment for various time duration at the fuel cell operation temperature (∼800 °C) for these glasses were found to generate mainly two different polymorphs celsian and hexacelsian during the entire heat treatment. The formation of undesirable celsian phase was retarded due to the high kinetic barrier associated with the transformation from hexacelsian to celsian. The developed glasses could be sealed at a temperature as low as 850 °C that helps to reduce the oxidation of ferritic steel interconnect used in anode-supported SOFC. Based on the physical properties, microstructure and the best sealing behavior with metal as well as electrolyte, the glass composition was optimized which has a very high resistivity of $\sim 3.75 \times 10^5$ Ωcm at the SOFC operating temperature (800 °C).

Acknowledgements

Financial support from Council of Scientific & Industrial Research (CSIR), under NMITLI Project is gratefully acknowledged. The authors are grateful to the director of this institute for giving permission to publish this work. Technical assistance from X-ray and SEM divisions of the institute is also acknowledged. The authors also acknowledge the input of Mr. S. Senthil Kumar for carrying out the dilatometry studies. SG is thankful to CSIR for providing senior research fellowship.

References

1. Taniguchi, S., Kadowaki, M., Yaseu, T., Akiyama, Y., Miyake, Y. and Nishio, K., Improvement of thermal cycle characteristics of a planar-type solid oxide fuel cell by using ceramic fiber as sealing material. *J. Power Sources*, 2000, **90**, 163–169.
2. Nguyen, B. C., Lin, T. A. and Mason, D. M., Electrocatalytic reactivity of hydrocarbons on a zirconia electrolyte surface. *J. Electrochem. Soc.*, 1986, **133**(9), 1807.
3. Sohn, S. B., Choi, S. Y., Kim, G. H., Song, H. S. and Kim, G. D., Stable sealing glass for planar solid oxide fuel cell. *J. Non-cryst. Solids*, 2002, **297**, 103–112.
4. Basu, R. N., *Materials for Solid Oxide Fuel Cells in Recent Trends in Fuel Cell Science and Technology*. Jointly published by Anamaya Publisher, New Delhi (India) and Springer, New York, 2006 (Chapter 12, 284–329).
5. Singhal, S. and Kendall, K., *High Temperature Solid Oxide Fuel Cells: Fundamentals, Design and Applications*. Elsevier, UK, 2003.
6. Basu, R. N., Blass, G., Buchkremer, H. P., Stöver, D., Tietz, F., Wessel, E. and Vinke, I. C., Simplified processing of anode-supported thin film planar solid oxide fuel cells. *J. Eur. Ceram. Soc.*, 2005, **25**(4), 463–471.
7. Basu, R. N., Das Sharma, A., Dutta, A., Mukhopadhyay, J. and Maiti, H. S., Development of anode-supported planar SOFC using inexpensive and simple processing technique. *Electrochem. Soc. Trans.*, 2007, **7**(1), 227–234.
8. Ley, K. L., Krumpelt, M., Kumar, R., Meiser, J. H. and Bloom, I., Glass ceramic sealants for SOFCs: Part I. Physical properties. *J. Mater. Res.*, 1996, **11**(6), 1489–1493.
9. Eichler, K., Solow, G., Otschik, P. and Schaffrath, W., BAS glasses for high temperature applications. *J. Eur. Ceram. Soc.*, 1999, **19**, 1101–1104.
10. Sohn, S. B., Oh, S. H., Choi, S. Y., Kim, G. H. and Seng, H. S., Preparation and characterization of sealing glass for SOFC. *J. Korean Ceram. Soc.*, 2001, **38**(2), 158–165.
11. Larsen, P. H. and James, P. F., Chemical stability of MgO/CaO/Cr_2O_3–Al_2O_3–B_2O_3–phosphate glasses in SOFC environment. *J. Mater. Sci.*, 1998, **33**, 2499–2507.
12. Horita, T., Sakai, N., Kawada, T., Yokokawa, H. and Dokiya, M., Reaction of SOFC components with sealing materials. *Denki Kagaku*, 1993, **61**(7), 760–762.
13. Yamamoto, T., Itoh, H., Mori, M., Mori, N. and Watanbe, T., Compatibility of mica glass ceramics as gas sealing materials for SOFC. *Denki Kagaku*, 1996, **64**(6), 575–581.
14. Akiyama, Y., Ishida, N., Murakami, S. and Saito, T., Solid oxide electrolyte fuel cell. US Patent 4,999,726, 1991.
15. Tiez, F., Thermal expansion of SOFC materials. *Ionics*, 1999, **5**, 129.
16. Larsen, P. H., Bagger, C., Mogensen, M. and Larsen, J., Stacking of plannar SOFCs. In *Proceedings of the 4th International Symposium on Solid Oxide Fuel Cells*. Electrochemical Society, Pennington, NJ, 1995, pp. 69–78, PV 95-1.
17. Lahl, N., Singheiser, L., Hilpart, K., Singh, K. and Bahadur, D., Aluminosilicate glass ceramics as sealant in SOFC stacks. In *Proceedings of the 6th International Symposium on Solid Oxide Fuel Cells*. Electrochemical Society, Pennington, NJ, 1999, p. 1057, PV 99–19.
18. Sohn, S. B. and Choi, S. Y., Suitable glass ceramic sealants for planar solid oxide fuel cells. *J. Am. Ceram. Soc.*, 2004, **87**(2), 254–260.
19. Zheng, R., Wang, S. R., Nie, H. W. and Wen, T. L., SiO_2–CaO–B_2O_3–Al_2O_3 ceramic glaze as sealant for planar ITSOFC. *J. Power Sources*, 2004, **128**, 165–172.
20. Brochu, M., Gauntt, B. D., Shah, R., Miyaka, G. and Loehnan, R. E., Comparison between barium and strontium glass composites for sealing SOFCs. *J. Eur. Ceram. Soc.*, 2005, **26**(15), 3307–3313.
21. Bahadur, D., Lahl, N., Singh, K., Singheiser, L. and Hilpart, K., Influence of nucleating agents on the chemical interaction of MgO–Al_2O_3–SiO_2–B_2O_3 glass sealants with components of SOFC. *J. Electrochem. Soc.*, 2004, **151**(4), A558–A562.
22. Goel, A., Tulyaganov, D. U., Agathopoulos, S., Ribeiro, M. J., Basu, R. N. and Ferreira, J. M. F., Diopside-Ca-Tschermak clinopyroxene based glass–ceramics processed via sintering and crystallization of glass powder compacts. *J. Eur. Ceram. Soc.*, 2007, **27**, 2325–2331.
23. Yang, Z., Stevenson, J. W. and Meinhardt, K. D., Chemical interaction of barium–calcium–aluminosilicate-based sealing glasses with oxidation resistant alloys. *Solid State Ionics*, 2003, **160**, 213–225.
24. Hanappel, V. A. C., Shemet, V., Vinke, I. C., Gross, S. M., Koppitz, Th., Menzler, N. H., Zahid, M. and Quadakkers, W. J., Evaluation of suitability of various glass sealants-alloy combinations under SOFC stack conditions. *J. Mater. Sci.*, 2005, **40**, 1583–1592.
25. Hanappel, V. A. C., Shemet, V., Gross, S. M., Koppitz, Th., Menzler, N. H., Zahid, M. and Quadakkers, W. J., Behaviour of various glass–ceramic sealants with ferritic steels under simulated SOFC stack conditions. *J. Power Sources*, 2005, **150**, 86–100.
26. Batfalsky, P., Hanappeal, V. A. C., Malzbender, J., Menzler, N. H., Shemet, V., Vinke, I. C. and Steinbrech, R. W., Chemical interaction between glass–ceramic sealants and interconnect steels in SOFC stacks. *J. Power Sources*, 2006, **155**(2), 128–137.
27. Ghosh, S., Das Sharma, A., Kundu, P., Basu, R. N. and Maiti, H. S., Tailor-made BaO–CaO–Al_2O_3–SiO_2 based glass sealant for anode-supported planar SOFC. *Electrochem. Soc. Trans.*, 2007, **7**(1), 2443–2452.
28. Volf, M. B., *Chemical Approach to Glass, Series on Glass Science and Technology, vol. 7*. Elsevier, New York, 1984.

29. Matveev, M. A., Matveev, G. M. and Frenkel, B. N., *Calculation and Control of Chemical, Optical and Thermal Properties of Glass*. Holon, Israel, 1975.
30. Vogel, W., *Glass Chemistry*. Springer-Verlag, 1992.
31. Wang, R., Lu, Z., Liu, C., Zhu, R., Huang, X., Wei, B., Ai, N. and Su, W., Characteristics of a SiO_2–B_2O_3–Al_2O_3–BaO–PbO_2–ZnO glass–ceramic sealant for SOFCs. *J. Alloys Compounds*, 2007, **432**(1–2), 189–193.
32. Bondi, A., *Physical Properties of Crystals, Liquids and Glasses*. John Wiley & Sons, 1968.
33. Beaman, R. G., Relation between (apparent) second-order transition temperature and melting point. *J. Polym. Sci.*, 1952, **9**, 470.
34. Sakka, S. and Mackenzie, J. D., Relation between apparent glass transition temperature and liquidus temperature for inorganic glasses. *J. Non-Cryst. Solids*, 1971, **6**, 145.
35. Lara, C., Pascual, M. J. and Duran, A., Glass forming ability, sinterability and thermal properties in the systems RO–BaO–SiO_2 (R = Mg, Zn). *J. Non-Cryst. Solids*, 2004, **348**, 149–155.
36. Blum, L., Fleck, R. and Jansing, T., High, Temperature fuel cell and high temperature fuel cell stack. US Patent 6165632, 2000.
37. Hyatt, M. J. and Bansal, N. P., Crystal growth kinetics in BaO–Al_2O_3–SiO_2 and SrO–Al_2O_3–$2SiO_2$ glasses. *J. Mater. Sci.*, 1996, **31**, 172–184.
38. Drummond, C. H., Lee, W. E., Bansal, N. P. and Hyatt, M. J., Crystallization of barium–aluminosilicate glass. *Ceram. Eng. Sci. Proc.*, 1989, **10**(9–10), 1485–1502.
39. Lara, C., Pascal, M. J., Prado, M. O. and Duran, A., Sintering of glasses in the system RO–Al_2O_3–BaO–SiO_2 (R = Ca, Mg, Zn) studied by hot-stage microscopy. *Solid State Ionics*, 2004, **170**, 201–208.